Zinc Removal from Basic Oxygen Steelmaking Filter Cake by Leaching with Organic Acids

JINGXIU WANG, ZHE WANG, ZHONGZHI ZHANG, and GUANGQING ZHANG

The dust generated from the basic oxygen steelmaking (BOS) process is a waste material mainly containing iron that cannot be recycled owing to its high zinc content. In this study, the leaching effects of different organic acids are compared, with the aim of determining an acid that selectively leaches and removes zinc from BOS dust, so that the waste material can be recycled into ironmaking and steelmaking processes in order to substitute part of the raw materials of steelmaking. The dust used in this study was scrubbed and collected in the form of a filter cake. The acids tested were oxalic, citric, acetic, propionic, butyric, and valeric acids. Butyric acid was found to be the most effective, with a high zinc extraction level of 49.7 pct and a low iron level of only 2.5 pct. Oxalic acid was the least effective leaching reagent for both zinc and iron extractions, owing to the formation of zinc and iron oxalate precipitates following metal dissolution. The filter cake and leached residues were characterized by chemical analysis, X-ray diffraction, X-ray photoelectron spectroscopy, and scanning electron microscopy with energy dispersive spectroscpopy.

https://doi.org/10.1007/s11663-018-1440-3
© The Minerals, Metals & Materials Society and ASM International 2018

I. INTRODUCTION

THERE are three main types of dusts generated in the steelmaking process, namely blast furnace (BF) dusts, basic oxygen steelmaking (BOS) dusts, and electric arc furnace (EAF) dusts. In terms of the BOS dust, it is a waste material comprising approximately 7 to 15 kg/t of produced steel in the steelmaking industry. It is estimated that 5 to 7 million tons of BOS dust are generated worldwide annually.[1,2] The dust is collected from the BOS off-gas either in the form of dry dust by dry separation methods, or in the form of sludge or filter cake from wet separation methods. Typically the off-gas is ducted to scrubbers for cleaning in order to dewater the collected dust for stockpiling (or further processing) as BOS filter cake.[3] The BOS dust contains high amounts of Fe, Zn, and other harmful elements like Pb, Cd, Cr, Ni, and Mn, which is usually classified as hazardous waste.[4] It presents an environmental issue, if it is not recycled, owing to its heavy metal constituents. This waste material cannot be recycled because of its high zinc content (1 to 4 pct), since zinc in the BOS dust recirculates in the plants, causing refractory failure and scaffold formation.[5,6]

The recycling of BOS dust plays an important role in the sustainability of the steelmaking industry, both environmentally and economically.[7] Typically, the zinc level in the dust is too low to be recovered economically by external processors, but the high iron levels and environmental burden of disposal make it worth recycling in steelmaking.[8,9] The recovery of iron from the dust at an acceptable zinc content level is an attractive option, if it can be achieved economically. It has been proposed that zinc could be directly recycled in the steelmaking process, as long as the final zinc content is below 0.4 pct.[10,11] The dust is stockpiled for lengthy periods, and large amounts are accumulated, which not only occupies valuable land, but also causes increasing environmental concern. The recycling of waste following the removal of zinc from BOS dust is becoming a pressing topic in the steelmaking industry.

Hydrometallurgical processing is a type of conventional process for metal recovery from a variety of solid materials, and is becoming an important process to deal with waste material in metallurgical industries.[12,13] These processes involve acid leaching, alkaline leaching, and bioleaching. Although certain strong inorganic acids, including sulfuric and hydrochloric acids, have been tested, these are generally less selective and result in the issue of new waste. Using weak inorganic acids such as phosphoric or carbonic acid for the selective leaching of zinc has rarely been reported in the literature. Steer

JINGXIU WANG and GUANGQING ZHANG are with the School of Mechanical, Materials, Mechatronic and Biomedical Engineering, University of Wollongong, Wollongong, NSW 2522, Australia. Contact e-mail: jw071@uowmail.edu.au ZHE WANG is with the State Key Laboratory of Advanced Metallurgy, University of Science and Technology Beijing, Beijing 100083, China. ZHONGZHI ZHANG is with the State Key Laboratory of Heavy Oil Processing, Faculty of Chemical Engineering, China University of Petroleum, Beijing 102249, China.

This study has patent pending for the technique employed.
Manuscript submitted August 2, 2018.
Article published online October 30, 2018.

and Griffiths[14] used 1.0 M phosphoric acid to leach zinc from BF dust slurry. Although 93 pct of zinc was extracted at a solid/liquid (S/L) ratio of 1:10 at ambient temperature for 24 hours, up to 21 pct of iron was also dissolved. Carbonic acid cannot be used in zinc leaching because of the low solubilities of CO_2 and $ZnCO_3$ in water. The use of organic acids for the leaching of waste materials offers advantages because these are biodegradable and environmentally benign, so the generation of secondary wastes can be avoided. They can potentially be obtained by the biodegradation of organic matter, such as the organic contaminants present in wastewater. Investigation into the leaching by organic acids will also provide information for the development of a potential bioleaching technology in the future.

Organic acids have been demonstrated as being effective in the leaching of certain other waste materials. Previous findings on the acid leaching of zinc and iron from wastes and their recovery are summarized in Table I.[14–17] Nagib and Inoue[17] dissolved 62 and 97 pct zinc from primary fly ash (PFA) and secondary fly ash (SFA), respectively. Effective selectivity of zinc over iron was achieved, which was closely related to the presence of Zn as amorphous compounds in the PFA, and zinc oxide in the SFA. It was noted that the acid usage was 100 times the stoichiometric acid amount in the PFA leaching and two times the amount in the SFA leaching. From Table I, it can be concluded that numerous important factors influence the selectivity of zinc leaching from waste materials, such as the contents and existing forms of zinc and iron, pH value of the acid solution, acid amount, and products of surface reactions. This is probably why different researchers have observed varying leaching behaviors of zinc and iron by means of oxalic and citric acid in previous studies. A systematic investigation has not been performed on the selective leaching of zinc from BOS dust using organic acids.

In order to utilize the value of the iron in the BOS dust while avoiding zinc accumulation in the steelmaking processes, zinc must be removed from the dust selectively. To achieve this, a suitable lixiviant that selectively leaches zinc is of paramount significance. Oxalic acid, citric acid, acetic acid, propionic acid, butyric acid, and valeric acid were tested for their individual effectiveness in the selective leaching of zinc from a sample of BOS dust in the form of a filter cake following water scrubbing and filtration with the aim of identifying a promising acid to maximize zinc recovery, while simultaneously minimizing iron removal. The initial BOS filter cake sample and leached residues were also characterized in order to understand the leaching behaviors of zinc and iron from the dust.

Table I. Previous studies on the Selective Leaching of Zinc from Waste Materials[14–17]

References	Sample	Composition (Pct)		Leaching Conditions	Leaching Efficiency (Pct)	
		Zn	Fe		Zn	Fe
14	blast furnace (BF) dust slurry	0.60	36.2	1.0 M oxalic acid, L/S = 10, room temperature, 24 h	18.5	31.2
15	low grade black shale ore	0.003	0.38	0.08 M oxalic acid, S/L = 1 pct (w/v), 30 days	35.2	—
				0.05 M citric acid, S/L = 1 pct (w/v), 30 days	14.5	—
16	municipal solid waste (MSW) incinerator fly ash	0.63	0.52	0.1 M oxalic acid, S/L = 1 pct (w/v), 30 °C, 120 rpm	86	48
				0.5 M oxalic acid, S/L = 1 pct (w/v), 30 °C, 120 rpm	68	51
				0.1 M citric acid, S/L = 1 pct (w/v), 30 °C, 120 rpm	83	27
				0.5 M citric acid, S/L = 1 pct (w/v), 30 °C, 120 rpm	70	19
17	primary fly ash (PFA)	0.80	1.37	3.3 M acetic acid, L/S = 7 mL/g, 30 °C, 60 min	62	8
	secondary fly ash (SFA)	40.2	2.12	3.3 M acetic acid, L/S = 7 mL/g, 30 °C, 60 min	97	42

II. EXPERIMENTAL

A. *Materials*

Leaching acid solutions were prepared using the above acids diluted with deionized water. Nitric acid was used to prepare the solutions for metal concentration analysis. All the chemicals and reagents used in this study were of analytical grade, and were purchased from Merck and Sigma-Aldrich Chemical Co. (St Louis, MO).

The filter cake sample was supplied by a local steelwork in Australia and extracted from the BOS steelmaking operation. The sample was first dried at 105 °C overnight to remove moisture and then crushed and screened to various particle size ranges. Crushed filter cakes within the size range of 300 to 500 μm were used in the leaching experiments.

B. *Acid Leaching*

The acid-leaching experiments were carried out in 250 mL Erlenmeyer flasks with 150 mL acid solutions on a horizontally oscillating shaker (RM2, Ratek, Australia) operated at 120 rpm, at room temperature. For the simpler and easier comparison of the effectivenesses of the acids on the selective leaching of zinc, the acid concentration was selected at 1.0 M, and the added mass of filter cake was expressed as "stoichiometric acid ratio" at 70 pct. The total leaching time was fixed at 10 hours, and acid solution samples were obtained at intervals for metal analysis and pH measurement. Metal analyses were carried out in 2 pct (w/w) nitric acid, using inductively coupled plasma optical emission spectroscopy (ICP-OES 710, Agilent Technologies, Australia). The pH of the acid solution was measured by a pH meter (PHSJ-4A, Shanghai Leici, China). The leaching residue at the end of the experiment was filtered, washed, dried, weighed, and subjected to further characterization.

The stoichiometric acid ratio is defined as the ratio of the actual amount of an acid to that theoretically consumed by Formula [1] for a complete zinc and iron reaction under an assumption of Fe and Zn presence as FeO and ZnO, respectively.

$$\mathrm{FeO/ZnO} + 2/x\mathrm{H}_x\mathrm{A} = \mathrm{FeA}_{2/x}/\mathrm{ZnA}_{2/x} + \mathrm{H_2O}, \quad [1]$$

where x is the highest valence number when the acid is fully dissociated.

The stoichiometric acid ratio following Formula [1] is calculated using the following equation:

$$\text{Stoichiometric acid ratio (Pct)} = \frac{\text{mol of acid} \times x}{2 \times (\text{mol of Fe and Zn in solid})} \times 100 \quad [2]$$

C. *Characterization of Raw Materials and Leached Residues*

The chemical composition of the BOS filter cake was determined by X-ray fluorescence (XRF) spectrometry. The original filter cake and leached samples were analyzed by X-ray diffraction (XRD, GBC-MMA, Australia) in order to determine their phase compositions. The analysis was implemented at 35 kV and 28.5 mA with monochromated Cu-Kα X-ray radiation (λ = 1.5406 Å) from 15 to 85 deg at a scanning speed of 1.5 deg/min and step size 0.05 deg. The samples were packed into a flat aluminum tray, and the surface was pressed flat.

The surface morphology of the BOS filter cake was analyzed by scanning electron microscopy (SEM, JEOL JSM-6490 LV). In order to gain further knowledge of the structure, morphology, and elemental distribution of the samples, certain sample particles were mounted with epoxy resin, and the ground and polished sections were carbon coated and then analyzed by scanning electron microscopy with energy dispersive spectroscopy (SEM/EDS). The analysis was performed at an accelerating voltage of 15 kV and the working distance was 10 mm.

X-ray photoelectron spectroscopy (XPS, SPECS PHOIBOS 100 Analyzer) was used to characterize the chemical states of the elements on the filter cake surface. A powdered sample was attached to an adhesive carbon tape inside an Ar glove box and then placed in a sealed container to reduce oxidation during transportation from the glove box to the XPS apparatus. The examination was conducted in a high-vacuum chamber with a residual pressure below 10^{-8} mbar. X-ray excitation was provided by Al Kα radiation (1486.6 eV) at a high voltage of 12 kV and power 120 W. The measurements were performed with the analyzer in the fixed transmission mode at a pass energy of 20 eV. XPS peak fitting was carried out using the CasaXPS 2.3.15 software package. All the spectra were calibrated via C 1s at 284.6 eV, and the background was corrected using linear approximation.

III. RESULTS AND DISCUSSION

A. *Characterization of the Original BOS Filter Cake*

Table II displays the chemical compositions of the sieved components for different particle size ranges, obtained by XRF, which demonstrates that the composition was uniform and without segregation owing to crushing and screening of the filter cake. Among the metals contained, the amounts of Fe, Zn, and Ca were significant, and the other metal contents were below 2 pct. The filter cake contained an average of 6.5 pct zinc and 56.4 pct iron. Furthermore, the sample contained 1.5 pct of carbon, as determined by combusting the carbonaceous materials in oxygen at 900 °C and monitoring the CO_2 amount released from the combustion.

Table II. Major Chemical Compositions (pct) of the BOS Filter Cake Crushed and Sieved to Different Particle Size Ranges

Size Range (μm)	Fe	Zn	SiO_2	Al_2O_3	CaO	Mn	MgO	TiO_2	K_2O	LOI
< 150	56.4	6.44	1.46	0.13	4.13	0.66	1.94	0.053	0.057	1.68
150 to 300	56.4	6.60	1.37	0.083	4.01	0.68	2.01	0.047	0.053	1.81
300 to 500	56.6	6.54	1.36	0.045	3.87	0.67	1.86	0.043	0.052	1.86
500 to 1000	56.3	6.48	1.45	0.11	3.92	0.67	1.91	0.046	0.053	2.20
1000 to 3350	56.4	6.56	1.42	0.088	3.88	0.67	1.96	0.047	0.051	1.91
> 3350	56.2	6.51	1.36	0.050	3.99	0.67	1.89	0.045	0.051	1.88

LOI, loss on ignition at 1050 °C.

Figure 1 illustrates the XRD pattern of the original filter cake sample. The analysis indicates that the BOS filter cake consisted of metallic iron, wüstite (FeO), magnetite (Fe_3O_4), zinc ferrite ($ZnFe_2O_4$), zinc oxide (ZnO), calcite ($CaCO_3$), and graphite. Wüstite is obviously the prominent phase, followed by iron and magnetite. The ZnO and $ZnFe_2O_4$ contents according to quantitative XRD were estimated to be equivalent to approximately 3 pct of zinc in the filter cake, which was significantly lower than that measured by XRF. Because XRF is a widely accepted method for metal oxide analysis, the discrepancy between the XRF and XRD data can be attributed to the formation of solid solutions between ZnO and FeO, or $ZnFe_2O_4$ and Fe_3O_4, or both. The main problem in zinc leaching is that $ZnFe_2O_4$ is known to be very stable and difficult to dissolve by simply using acid or alkaline under moderate conditions.[18,19] The formation of solid solutions between the metal oxides is expected to stabilize zinc further in the mineral phases, which makes leaching this zinc more challenging.

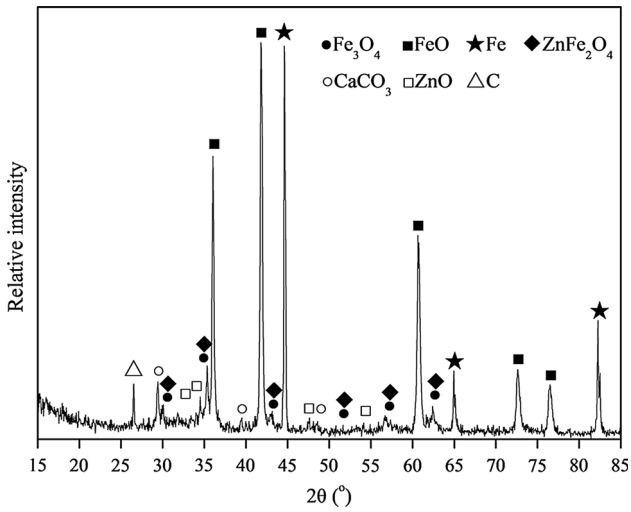

Fig. 1—XRD pattern of the original BOS filter cake.

Figure 2 presents the SEM images of the filter cake particles at magnifications ×150 and ×600, which illustrate the morphological characteristics of the BOS filter cake surface. The BOS filter cake particles are made up of various shapes and sizes, and the large particles were observed to be agglomerates of submicrometer particles, forming a porous structure, which was clarified in the SEM image at high magnification (×600).

The filter cake particles were mounted, sectioned, and further observed by SEM/EDS. Figure 3 illustrates a backscattered image of the filter cake sample, which contained a zinc-rich area, as well as the distributions of the major elements, including zinc, iron, oxygen, calcium, and magnesium, as observed by the EDS mapping. It can be seen from the SEM image in Figure 3 that the filter cake particles mainly consisted of fine iron oxide grains of less than 1 μm; the fraction of grains larger than 1 μm was small. Voids existed between the grains, which resulted in the particles having high porosity. In the zinc-rich area, the pores between the iron oxide grains were filled with zinc oxide. It should be noted that zinc-rich areas, such as those in Figure 3, are rarely found, while those with zinc-enriched grains and smaller areas, with a lower zinc content, are more common. The EDS point analysis also demonstrated that zinc was distributed uniformly on the surface of the iron oxide grains, which is not obvious in Figure 3.

Apart from iron and zinc oxides, the major impurities in the filter cake included calcium, magnesium, and silicon oxides. From Figure 3, it is seen that CaO and MgO co-existed in the large zinc-rich zone, but were separated from one another because the bright areas in their EDS mappings were complementary. Furthermore, the calcium oxide existed as segregated particles, which may be a result of the dust generated from the limestone flux during slag forming.

XPS analyses were carried out in order to further investigate the zinc and iron chemical states in the BOS filter cake. Figure 4(a) illustrates the overall energy spectrum of the sample, in which zinc, iron, oxygen, and carbon existed, as expected. The high-resolution XPS fine spectra of the Zn 2p, Fe 2p, and O 1s peaks are

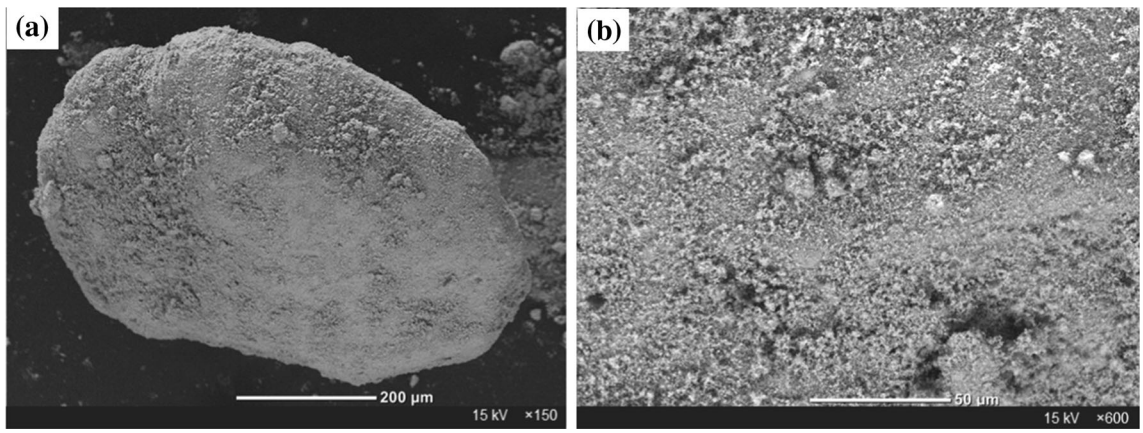

Fig. 2—Surface morphology of BOS filter cake particles, as observed by SEM at different magnifications: (*a*) ×150; and (*b*): ×600.

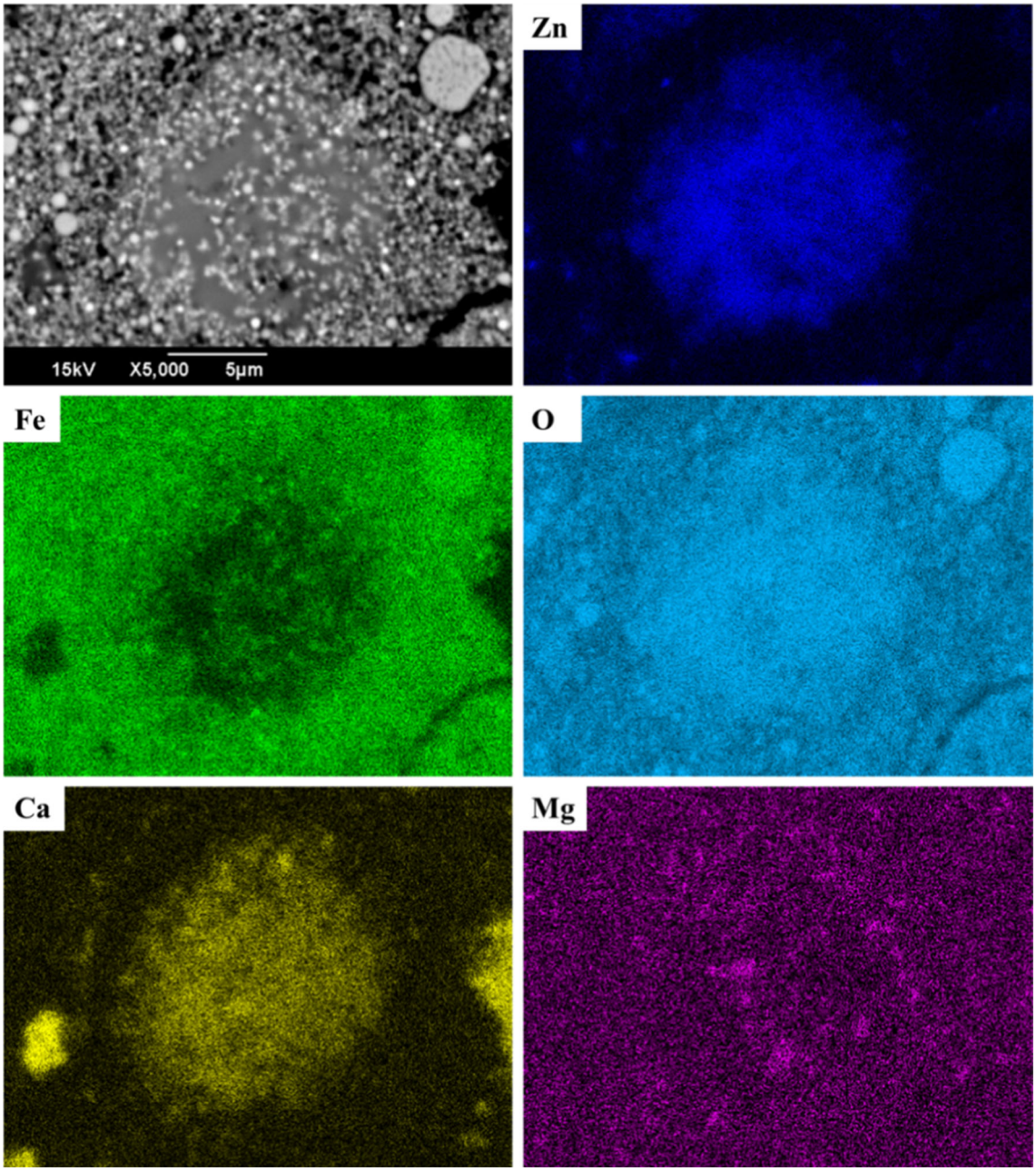

Fig. 3—EDS mapping of the elemental composition of the original BOS filter cake.

displayed in Figures 4(b), (c), and (d), respectively. Table III compares the peak positions obtained in the current study with the results reported in the literature.[20–23]

In Figure 4(b), the Zn $2p_{3/2}$ photoelectron peak at 1020.8 eV and Zn $2p_{1/2}$ at 1043.8 eV with a peak separation of 23.0 eV reveal the Zn^{2+} oxidation state in the sample.[20] The peak of the Zn $2p_{3/2}$ electrons is split into two components with binding energies (BEs) of 1018.2 and 1020.8 eV, which are probably ascribed to $ZnFe_2O_4$ and ZnO, with a peak area ratio of 4.39:1.[21] As a surface analysis measure, the XPS data do not represent the bulk compositions. Figure 4(c) presents the Fe 2p peaks at the lower and higher BEs assigned to Fe $2p_{3/2}$ and Fe $2p_{1/2}$, respectively, accompanied by two corresponding satellite peaks with BEs of 718.2 and 731.9 eV.[22] The BE difference over 6 eV between the major and satellite peaks confirms the existence of Fe^{3+}.[23] Furthermore, it is observed that Fe $2p_{3/2}$ exhibits degeneracy of two states: Fe^{3+} and Fe^{2+}, with an area ratio of 0.54. However, the peak corresponding to Fe^0 was not detected, because the metallic iron grain surface was oxidized. The O 1s spectrum exhibits two fitting peaks in Figure 4(d). The peak located at 529.7 eV is typical of metal-oxygen bonds (Zn and Fe oxides) and the other peak at 531.0 eV is attributed to oxygen in the OH^- groups and carbonate species on the surface.[20,23]

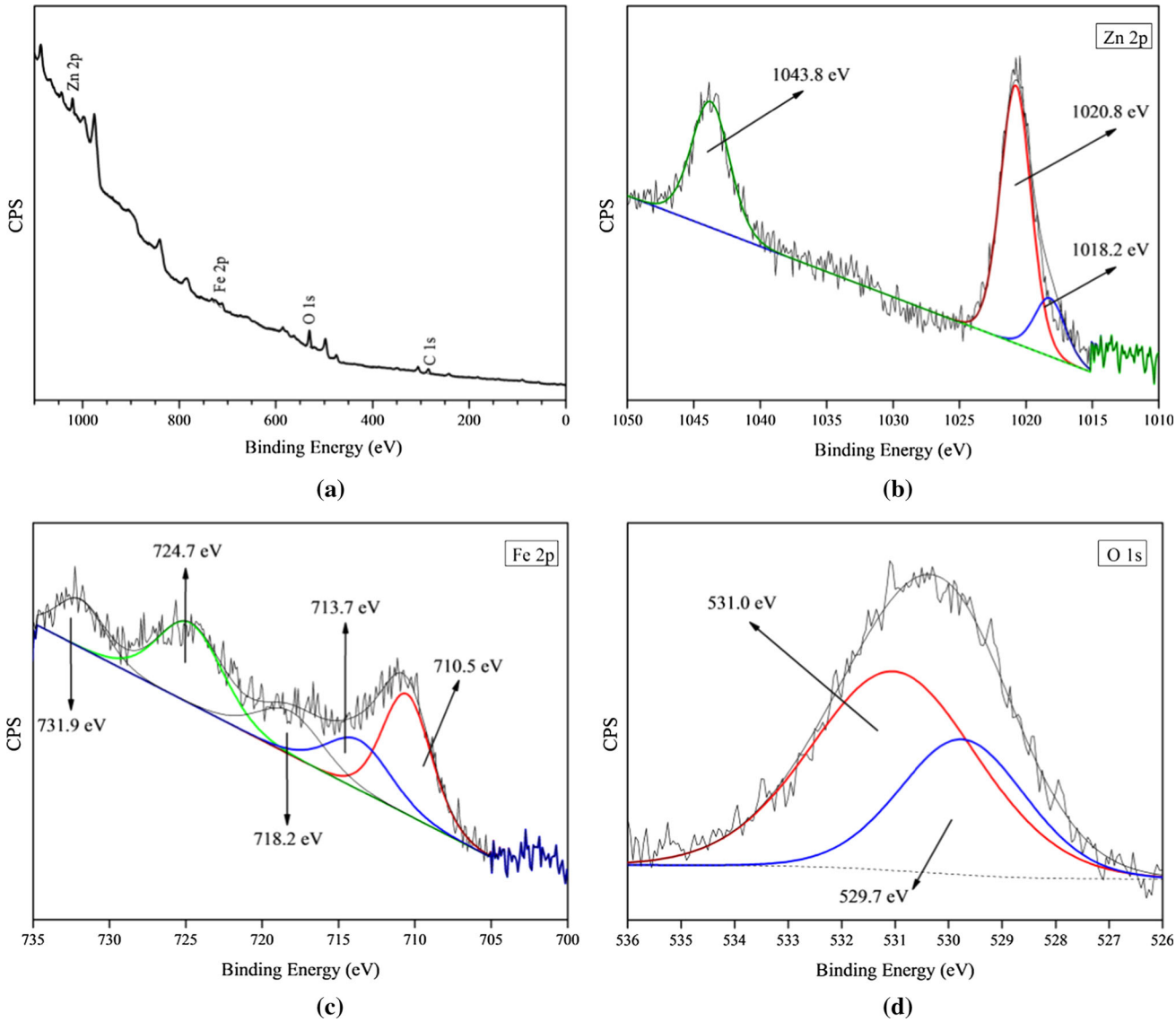

Fig. 4—High-resolution XPS patterns of the original BOS filter cake prior to leaching: (*a*) energy spectrum; (*b*) Zn 2p; (*c*) Fe 2p; and (*d*) O 1s.

It can be concluded from the XRD, SEM/EDS, and XPS analyses that the zinc in the BOS filter cake mainly existed as $ZnFe_2O_4$, ZnO, and solid solutions with iron oxides.

B. *Leaching Effects of Different Acids in the Removal of Zinc from Filter Cake*

The leaching efficiency was calculated as follows:

$$\text{Leaching efficiency (pct)} = \frac{\text{Mass of } M \text{ in leachate}}{\text{Mass of } M \text{ in the filter cake added into flask}} \times 100, \quad [3]$$

where M is either zinc or iron.

The leaching efficiencies of Fe and Zn depend on the type of acid used, the acid concentration and amount, the reaction time, and other process conditions. All experiments were carried out at ambient temperature, using a shaking rate of 120 rpm, for 10 hours.

Figure 5 compares the leaching efficiencies of zinc and iron from the BOS filter cake using various organic carboxylic acids under the conditions detailed above. It can be seen clearly that the acids showed various leaching behaviors of zinc and iron as a function of time. Butyric acid was the most effective leaching reagent, with 49.7 pct of zinc and only 2.5 pct of iron leached. Nearly half of zinc extraction at 23.2 pct was obtained within the first 20 min, followed by a gradual increase. Noted that the zinc extraction reached as high as 41.0 pct after 3 hours of leaching. Two acids with higher zinc extraction were acetic and propionic acid, extracting 57.3 and 52.8 pct of zinc, respectively. Unfortunately, 40.3 and 33.6 pct of iron were also correspondingly extracted from the sample. Both their zinc and iron dissolutions showed similar increasing trend with the leaching time. Valeric acid also exhibited a certain selectivity of zinc over iron, with 40.3 and 21.0 pct of zinc and iron extraction, respectively, but lower

Table III. Binding Energy (BE) and Peaks of the Different Elements in the BOS Filter Cake Compared to the Results from the Literature[20–23]

References	Sample	Element	Peak	BE (eV)
Current study	BOS filter cake	O	O1s	529.7, 531.0
		Fe	$2p_{3/2}$	710.5
			$2p_{1/2}$	724.7
		Zn	$2p_{3/2}$	1020.8, 1018.2
			$2p_{1/2}$	1043.8
20	$ZnFe_2O_4$ nanoelectrodes	O	O1s	529.6, 530.9
		Fe	$2p_{3/2}$	711.4
			$2p_{1/2}$	725.0
		Zn	$2p_{3/2}$	1021.4, 1045.2
			$2p_{1/2}$	—
21	$ZnFe_2O_4$ nanomagnets	O	O1s	529.6, 530.9
		Zn	$2p_{3/2}$	1021.8, 1021.5
			$2p_{1/2}$	—
22	zinc leaching residue	Fe	$2p_{3/2}$	711.1
			$2p_{1/2}$	724.8
		Zn	$2p_{3/2}$	1021.0, 1022.5
			$2p_{1/2}$	1044.4
23	$ZnFe_2O_4$ photocatalyst	O	O1s	529.5, 531.0
		Fe	$2p_{3/2}$	711.3
			$2p_{1/2}$	724.9
			satellite	718.5
		Zn	$2p_{3/2}$	1021.4;
			$2p_{1/2}$	1044.4

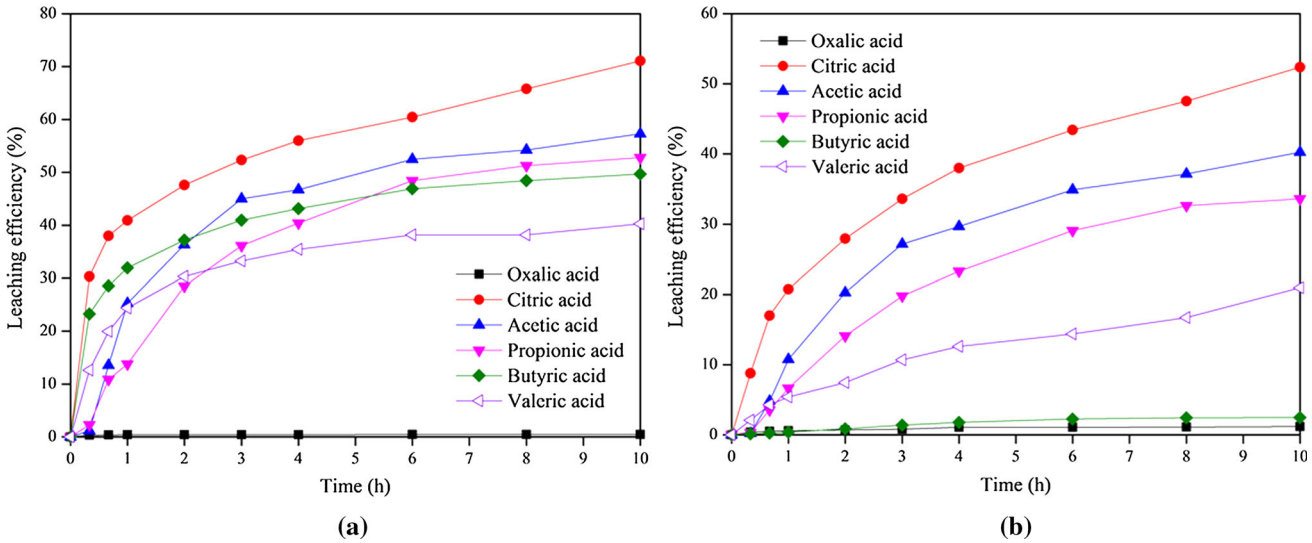

Fig. 5—Leaching efficiencies of (*a*) zinc and (*b*) iron from filter cake using different acids with 1.0 M concentration and 70 pct stoichiometric acid ratio at 120 rpm and room temperature.

leaching efficiency compared to the other alkyl acids illustrated above. Like butyric acid leaching, there was 33.3 pct of zinc removal after 3 hours despite that 10.7 pct of iron was also dissolved. As indicated, oxalic acid appeared to leach neither zinc nor iron because of the leaching efficiency of less than 1.5 pct for both the elements. Citric acid extracted the highest level of zinc, at 71.1 pct, but also exhibited the highest capacity of iron extraction, at 52.4 pct, making it unsuitable as a candidate for leaching the BOS filter cake. However, better selectivity of zinc over iron was achieved within the first 20 minutes with 30.3 and 8.8 pct of zinc and iron extractions, respectively. Thereafter, the selectivity became worse with faster iron dissolution but slower zinc dissolution.

Figure 6 shows the variations in pH with leaching time using various organic acids. The initial pH of oxalic acid solution was the lowest, although a slight increase was observed within the first 20 minutes, the pH remained almost constant thereafter. Acetic acid,

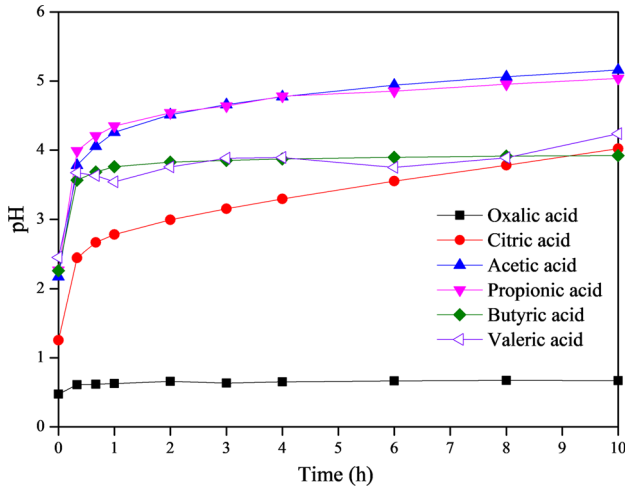

Fig. 6—pH variation with leaching time using various organic acids.

propionic acid, butyric acid, and valeric acid exhibited similar initial pH value within a narrow range 4.76 to 4.88, and fast increase of pH occurred within the first 20 minutes. The pH of both the acetic and propionic acid solutions gradually increased to approximately 5.2 after leaching for 10 hours. In comparison, smaller increase to 3.9 and 4.2 was observed for butyric acid and valeric acid, respectively. Citric acid solution showed a dramatic rise in pH from 1.2 to 4.0.

Table IV displays the chemical structure, acidity, and solubility (in water, at 25 °C) of the six different organic acids used in the study, the Ksp values of oxalate salts and the stability constants (log *K*) of various metal chelates.[24] The p*K*a values of the organic acids tested were in the opposite sequence with their acidities. As the number of carbons in the alkanoic acid series increased, the water solubility decreased (Table IV). The extraction of metals with organic acids has been reported to be related to their acidic as well as chelating characteristics.[25]

The leaching reactions presented as Formula [1] proceeded in the steps illustrated in Formulae [4] and [5].

$$RCOOH + H_2O \rightleftharpoons RCOO^- + H_3O^+ \quad [4]$$

$$2H_3O^+ + MO \rightleftharpoons M^{2+} + 3H_2O \quad [5]$$

Among the six acids, oxalic acid is the strongest, and has been widely used in the leaching of iron oxides, as it presents a lower risk of contamination of the treated materials following leaching, as well as exhibits effective complexing characteristics and high reduction power.[26,27] The negligible pH variation resulted in the low leaching efficiencies of zinc and iron. Although small amounts of iron and zinc were transferred to the liquid solution, the XRD analysis demonstrated that a high degree of reactions occurred between the filter cake and oxalic acid (Figure 8). Very low leaching efficiencies were determined by the ICP-OES analysis of the solution phase, because zinc and ferrous humboldtine exhibit low solubility in aqueous solutions at room temperature. Both the leaching products of zinc and iron oxalate precipitates can be formed based on their Ksp values, displayed in Table IV. Furthermore, iron oxalate is more soluble than zinc oxalate and precipitation may first take place by zinc oxalate,[28] which explains why the iron dissolution was greater than the zinc extraction. However, the leaching results do not agree with previous findings.[14,16] The high leaching efficiencies of zinc and iron in the previous publications are related to the differences in the amounts of acid used and the mass percentages of the zinc and iron contained (Table I). The significant formation of humboldtine explains the distinction of the oxalic acid leaching results from those in the literature.

Citric acid demonstrated the strongest ability in terms of the leaching of zinc and iron among the acids studied in the current study, and this capacity is related to its high acidity and excellent chelating role. Citric acid dissociates in three stages as follows:

$$C_6H_8O_7 + H_2O = H_3O^+ + C_6H_7O_7^- \quad [6]$$

$$C_6H_7O_7^- + H_2O = H_3O^+ + C_6H_6O_7^{2-} \quad [7]$$

$$C_6H_6O_7^{2-} + H_2O = H_3O^+ + C_6H_5O_7^{3-} \quad [8]$$

The acidity of the first-stage dissociation is between that of oxalic and acetic acid, and that of the second-stage dissociation is equivalent to that of acetic acid. The coordination of citric acid with the zinc and iron ions resulted in an increase in the sample solubility, which is consistent with the results of Irannajad *et al.*[29] for the citric acid leaching of low-grade oxide ores. Furthermore, the second and third dissociation further increased the citric acid chelating capacity. It was probably the chelating property that led to the higher leaching yield of zinc.[30] The improved selectivity of zinc over iron, reported by Wu and Ting[16] was probably related to the excess stoichiometric amount of acid.

The leaching results by means of acetic, propionic, butyric and valeric acid were influenced by more factors., The similar zinc and iron extractions for acetic acid, and propionic acid were probably caused by the similar pKa, initial pH and acidity changes. For the butyric acid solution, it appears that a smaller decrease in acidity facilitated the selective leaching of zinc over iron. The zinc leaching efficiency decreased with an increasing carbon number in the acid molecules, which can be mainly attributed to the structure difference of a methylene bridge (-CH_2-).[14] Unlikely, the leaching efficiency of iron decreased until butyric acid but further increasing the carbon number to valeric acid caused its increase. The deviation of the valeric acid leaching from the previous trend was caused by the lower solubility of valeric acid in water. Although the amount of valeric acid added into the leaching vessel was equivalent to 1.0 M, the dissolved valeric acid in the solution was below 0.5 M. The results indicate the evident synergistic effects

Table IV. Chemical Structure, Acidity, and Solubility (in Water, at 25 °C) of Different Organic Acids, Ksp Values of Oxalates, and the Stability Constants (log *K*) of Various Metal Chelates

Acid Name	Formula	p*K*a1	p*K*a2	p*K*a3	pH	Solubility (g/L)	Solubility Product Constant (Ksp) at 25 °C	Stability Constant (log *K*)		
								Zn^{2+}	Fe^{2+}	Fe^{3+}
Citric acid	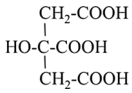	3.13	4.76	6.39	1.17	164	—	4.5	3.2	11.85
Oxalic acid	HOOC-COOH	1.25	4.14	—	0.42	143	$ZnC_2O_4{\cdot}2H_2O$: 1.38×10^{-9} $FeC_2O_4{\cdot}2H_2O$: 2.1×10^{-7}	4.9	>4.7	9.4
Acetic acid	H_3C-COOH	4.76	—	—	2.16	Miscible	—	1.03	—	—
Propionic acid	H_3C-CH_2-COOH	4.88	—	—	2.27	Miscible	—	1.01	—	3.45
Butyric acid	H_3C-$(CH_2)_2$-COOH	4.82	—	—	2.24	Miscible	—	1.00	—	—
Valeric acid	H_3C-$(CH_2)_3$-COOH	4.84	—	—	2.48	49.7	—	—	—	—

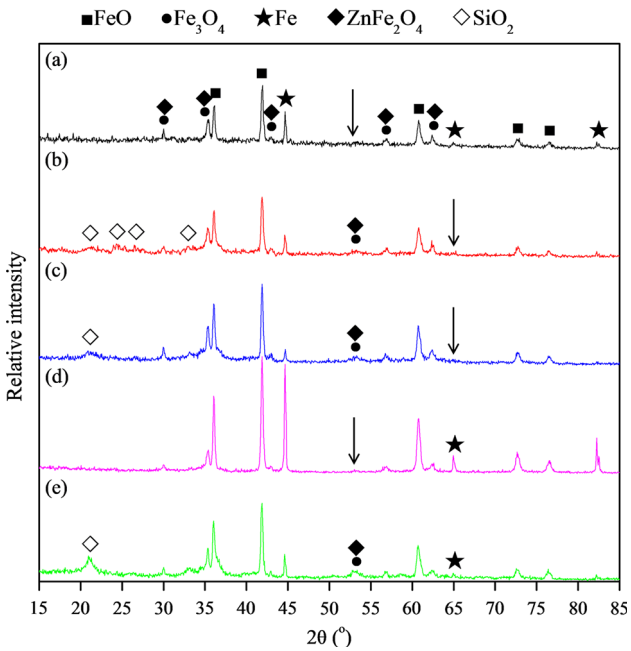

Fig. 7—XRD patterns of the residues leached by organic acids with 70 pct stoichiometric acid ratio and 1.0 M concentration. Leaching was carried out at 120 rpm and room temperature for 10 h: (*a*) citric acid; (*b*) acetic acid; (*c*) propionic acid; (*d*) butyric acid; and (*e*) valeric acid.

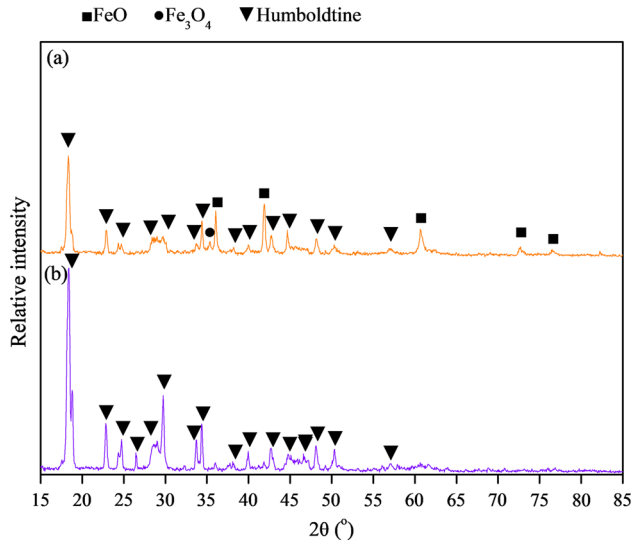

Fig. 8—XRD patterns of the oxalic acid residue leached at 70 pct stoichiometric acid ratio and 1.0 M concentration. Leaching was carried out at 120 rpm and room temperature for 10 h: (*a*) coarse particles; and (*b*) fine particles.

of acidity, structure, and solubility on the superior selectivity of zinc over iron when using butyric acid among the alkanoic acids.

Butyric acid was identified as a promising acid in the selective leaching of zinc from the BOS filter cake, taking account of its selectivity of zinc over iron at a ratio of 26.6. In comparison, the selectivity using traditional mineral acids at room temperature reported previously was relatively low mainly from higher iron dissolution. For example, Langová and Matýsek[31] showed a ratio of 5, while Kelebek *et al.*[1] achieved 4.5 and 15.8 for coarse and fines using H_2SO_4. There was a study with the selectivity lower than 5 for H_2SO_4, HNO_3, HCl, and H_3PO_4.[14] It should be noted that the selectivity of the mineral acids was generally improved by the elevated temperature.[32,33]. Therefore, maximum zinc and minimum iron extractions may be achieved by optimizing the butyric acid-leaching conditions in another study.

C. *Characterization of the Leached Residues*

The XRD pattern of the filter cake that was leached for 2 days using Milli-Q water alone was hardly changed, demonstrating that the natural leaching effect of the filter cake could be ignored. Except for the oxalic acid-leached residue, the XRD patterns of the other residues leached in the acids of 1.0 M concentration at a 70 pct stoichiometric acid ratio for 10 hours are presented in Figure 7.

According to Figure 7, the peaks of $CaCO_3$, graphite, and ZnO disappeared in all the XRD patterns of the acid-leached residues. It is understood that $CaCO_3$ reacted with the acids during leaching, releasing CO_2. The disappearance of the graphite peak could be owing to the adsorption of acid molecules on its surface causing separation of the graphite from the filter cake particles, following which the graphite particles were lost when the filter cake residue was separated from the liquid and then washed. ZnO was reported to be more easily dissolved in traditional acid leaching method in comparison with $ZnFe_2O_4$.[1] The iron-bearing phases of all the acid-leached residues remained the same as those of the original filter cake, but significant differences of the relative contents between Fe and FeO were observed. Butyric acid-leached residue showed no obvious changes, since the leaching mainly occurred for zinc rather than iron, while the major phases detected by the XRD analysis were iron-containing phases. The main peaks of the Fe and FeO became very weak in the other leached residues, and certain minor peaks even disappeared (indicated by ↓). This result is in strong agreement with the high leaching efficiency of iron in these acids.

The oxalic acid-leaching residue exhibited two obvious particle size ranges: the coarse particles originated from the original particles, while the fine particles were deported from the large ones. Hence, the oxalic acid-leaching residue was composed of two parts, namely deported fines and coarse particles. These were separated and analyzed individually by means of XRD in order to gain further information regarding the oxalic acid-leaching behavior. Their XRD patterns are presented in Figure 8.

In the coarse particles shown in Figure 8(a), only humboldtine (ferrous oxalate hydrate $FeC_2O_4{\cdot}2H_2O$) was identified from the fine particles of the oxalic acid-leached residues. In the coarse particles, humboldtine was detected as the major phase, together with certain amounts of wüstite and magnetite. No metallic iron peaks were identified in the leached residue, suggesting that the metallic iron was completely transformed into humboldtine. The precipitate was lime green and yellow, corresponding to the color of ferrous oxalate. No zinc oxalate was observed in the XRD analysis owing to the low content of the compound.

IV. CONCLUSIONS

The leaching of zinc and iron from a BOS filter cake was investigated using six organic acids in order to examine their capacity to leach zinc selectively over iron. The following conclusions are drawn from the investigation.

1. The original BOS filter cake was made up of submicron particles mainly consisting of wüstite, metallic iron, and magnetite. Zinc oxide was distributed on the iron oxide particles in different chemical states, including deposited ZnO between the particle gaps and on the particle surface, combined with iron oxide as $ZnFe_2O_4$, and solid solutions of FeO and Fe_3O_4. The formation of Zn-Fe oxide compounds and solid solutions made zinc oxide leaching difficult.
2. Among the organic acids tested, butyric acid exhibited excellent selectivity, with up to 49.7 pct of the zinc being leached from the filter cake. The leaching efficiency of iron was only 2.5 pct. Under the conditions of this investigation, the other acids could not leach zinc from the filter cake selectively. In oxalic acid, zinc and iron could not dissolve into the solution, while for the other acids, both zinc and iron were dissolved, with low or no selectivity.
3. In the leaching with oxalic acid, both zinc and iron oxalates were formed and precipitated, making the leaching inefficient. Citric acid exhibited the highest leaching efficiency for both zinc and iron. The zinc leaching efficiency decreased following the increased carbon numbers in the acid molecules, in the sequence: acetic acid > propionic acid > butyric acid > valeric acid. For iron, the leaching efficiency decreased similarly until the carbon number corresponded to that of butyric acid, and reached as low as 2.5 pct. However, the iron leaching efficiency by valeric acid increased to 21 pct.

ACKNOWLEDGMENTS

The authors acknowledge the awarding of the CSC scholarship by the China Scholarships Council and the IPTA scholarship by the University of Wollongong to Miss Jingxiu Wang. The BOS filter cake sample used in this work was supplied by BlueScope Steelmaking Ltd. The authors would like to thank Dr. Linda Tie and Dr. Dongqi Shi for their assistance in the ICP-OES and XPS analyses. The SEM/EDS and XPS analyses were completed at the Electron Microscopy Centre, University of Wollongong.

REFERENCES

1. S. Kelebek, S. Yörük, and B. Davis: *Miner. Eng.*, 2004, vol. 17, pp. 285–91.
2. J. Vereš, Š. Jakabský, and M. Lovás: *Miner. Slovaca*, 2010, vol. 42, pp. 369–74.
3. Z. Wang, D. Pinson, S. Chew, B.J. Monaghan, H. Rogers, and G. Zhang: *ISIJ Int.*, 2016, vol. 56, pp. 505–12.
4. M.L. Sammut, J. Rose, A. Masion, E. Fiani, M. Depoux, A. Ziebel, J.L. Hazemann, O. Proux, D. Borschneck, and Y. Noack: *Chemosphere*, 2008, vol. 70, pp. 1945–51.
5. P. Dvorak and J. Jandova: *Waste Forum*, 2002, vol. 6, pp. 22–24.
6. Z.H. Trung, F. Kukurugya, Z. Takacova, D. Orac, M. Laubertova, A. Miskufova, and T. Havlik: *J. Hazard. Mater.*, 2011, vol. 192, pp. 1100–07.
7. L.M. Wu: *Ironmak. Steelmak.*, 1999, vol. 26, pp. 372–77.
8. K. Gargul and B. Boryczko: *Arch. Civil Mech. Eng.*, 2015, vol. 15, pp. 179–87.
9. J. Steer, C. Grainger, A. Griffiths, M. Griffiths, T. Heinrich, and A. Hopkins: *Ironmak. Steelmak.*, 2014, vol. 41, pp. 61–66.
10. S.M. Smith, X. Zhou, and C.L. Nassaralla: *Iron Steelmak.*, 2000, vol. 27, pp. 69–76.
11. L. Wang, X. Lu, X. Wei, Z. Jiang, S. Gu, Q. Gao, and Y. Huang: *J. Anal. At. Spectrom.*, 2012, vol. 27, pp. 1667–73.

12. V. Montenegro, P. Oustadakis, P.E. Tsakiridis, and S. Agatzini-Leonardou: *Metall. Mater. Trans. B*, 2013, vol. 44B, pp. 1058–69.
13. H. Shalchian, A. Rafsanjani-Abbasi, J. Vahdati-Khaki, and A. Babakhani: *Metall. Mater. Trans. B*, 2014, vol. 46B, pp. 38–47.
14. J.M. Steer and A.J. Griffiths: *Hydrometallurgy*, 2013, vol. 140, pp. 34–41.
15. F. Anjum, H.N. Bhatti, M.A. Ghauri, I.A. Bhatti, M. Asgher, and M.R. Asi: *Afr. J. Biotechnol.*, 2009, vol. 8, pp. 5038–45.
16. H.Y. Wu and Y.P. Ting: *Enzyme Microb. Technol.*, 2006, vol. 38, pp. 839–47.
17. S. Nagib and K. Inoue: *Hydrometallurgy*, 2000, vol. 56, pp. 269–92.
18. J. Han, W. Liu, W. Qin, Y. Zheng, and H. Luo: *Metall. Mater. Trans. B*, 2016, vol. 47B, pp. 686–93.
19. T. Miki, R. Chairaksa-Fujimoto, K. Maruyama, and T. Nagasaka: *J. Hazard. Mater.*, 2016, vol. 302, pp. 90–96.
20. A.A. Tahir and K.U. Wijayantha: *J. Photochem. Photobiol. A*, 2010, vol. 216, pp. 119–25.
21. F. Pan, Y. Guo, F. Cheng, T. Fa, and S. Yao: *Chin. Phys. B.*, 2011, vol. 20, p. 127501.
22. M. Li, B. Peng, L. Chai, N. Peng, X. Xie, and H. Yan: *Trans. Nonferrous Met. Soc. China*, 2013, vol. 23, pp. 1480–88.
23. R. Dom, A.S. Chary, R. Subasri, N.Y. Hebalkar, and P.H. Borse: *Int. J. Energy Res.*, 2015, vol. 39, pp. 1378–90.
24. D.D. Perrin, B. Dempsey, and E.P. Serjeant: *pKa Prediction for Organic Acids and Bases*, 1st ed., Chapman & Hall, New York, 1981.
25. X.S. Jing, F.Q. Liu, X. Yang, P.P. Ling, L.J. Li, C. Long, and A.M. Li: *J. Hazard. Mater.*, 2009, vol. 167, pp. 589–96.
26. S.O. Lee, T. Tran, Y.Y. Park, S.J. Kim, and M.J. Kim: *Int. J. Miner. Process.*, 2006, vol. 80, pp. 144–52.
27. D. Panias, M. Taxiarchou, I. Paspaliaris, and A. Kontopoulos: *Hydrometallurgy*, 1996, vol. 42, pp. 257–65.
28. I. De Michelis, F. Ferella, E. Karakaya, F. Beolchini, and F. Veglio: *J. Power Sources*, 2007, vol. 172, pp. 975–83.
29. M. Irannajad, M. Meshkini, and A.R. Azadmehr: *Physicochem. Probl. Min. Process.*, 2013, vol. 49, pp. 547–55.
30. M.D. Del and S. Babel: *Water Sci. Technol.*, 2006, vol. 54, pp. 129–35.
31. Š. Langová and D. Matýsek: *Hydrometallurgy*, 2010, vol. 101, pp. 171–73.
32. T. Havlik, B. Friedrich, and S. Stopić: *Erzmetall*, 2004, vol. 57, pp. 113–20.
33. J. Vereš, Š. Jakabský, and M. Lovás: *Acta Mont. Slovaca*, 2011, vol. 16, pp. 185–91.